Low Frequency Electrorotation of Fixed Red Blood Cells

R. Georgieva,*# B. Neu,* V. M. Shilov,§ E. Knippel,¶ A. Budde,¶ R. Latza,* E. Donath,= H. Kiesewetter,* and H. Bäumler*

*Institute of Transfusion Medicine and Immunohematology, Charité, Humboldt-University of Berlin, D-10098 Berlin, Germany, #Thrakia University, Medical School, Department of Physics and Biophysics, Stara Zagora, Bulgaria, §Institute of Biocolloid Chemistry, Kiev, Ukraina, ¶Department of Internal Medicine, Laboratory for Special Measuring Techniques, University of Rostock, Germany, and =Max-Planck-Institute of Colloids and Interfaces, Berlin, Germany

ABSTRACT Electrorotation of fixed red blood cells has been investigated in the frequency range between 16 Hz and 30 MHz. The rotation was studied as a function of electrolyte conductivity and surface charge density. Between 16 Hz and 1 kHz, fixed red blood cells undergo cofield rotation. The maximum of cofield rotation occurs between 30 and 70 Hz. The position of the maximum depends weakly on the bulk electrolyte conductivity and surface charge density. Below 3.5 mS/m, the cofield rotation peak is broadened and shifted to higher frequencies accompanied by a decrease of the rotation speed. Surface charge reduction leads to a decrease of the rotation speed in the low frequency range. These observations are consistent with the recently developed electroosmotic theory of low frequency electrorotation.

INTRODUCTION

Electrorotation is a dielectric spectroscopy technique for the characterization of dispersed colloids and biocolloids. The general cause of the particle rotation is a phase difference between the electric field-induced polarization and the external rotating field (Arnold and Zimmermann, 1988; Fuhr, 1985). This gives rise to a torque acting upon the particle. From the absolute value and the phase of the particle's induced dipole moment together with the hydrodynamic friction, the rotation speed is calculated. Likewise, the dielectric dispersion of suspensions can be obtained from the characteristics of the particle's induced dipole moment (Dukhin and Shilov, 1974). Thus, both phenomena seem to be equivalent. A rigid correlation between electrorotation and the dielectric dispersion of a suspension of the same particles should exist (Arnold et al., 1987; Wang et al., 1993). This line of reasoning is in good agreement with many experimental findings at higher field frequencies (Arnold and Zimmermann, 1982; Pastushenko et al., 1985; Arnold et al., 1987; Donath et al., 1990; Müller et al., 1993; Wang et al., 1993; Zhou et al., 1995; Sukhorukov and Zimmermann, 1996; Gimsa et al., 1996; Burt et al., 1996). The equivalency between electrorotation and impedance measurements at high frequencies means that the information, which can be obtained by booth methods, is equivalent. The advantage of electrorotation is that dielectric properties of single particles can be studied.

If the particle is inhomogeneous with regard to its electric and dielectric parameters, several minima and maxima can be observed in an electrorotation spectrum, each one corresponding to a specific dispersion process. It has been shown that this method is especially suitable to study the biological cell membrane and cell interior dielectric properties (Arnold and Zimmermann, 1982; Donath et al., 1990; Müller et al., 1993; Wang et al., 1994; Egger and Donath, 1995; Huang et al., 1995; Sukhorukov and Zimmermann, 1996; Gimsa et al., 1996). The corresponding frequency range falls in the kHz to MHz region and is called β-dispersion. The underlying concepts have been frequently discussed (Pauly and Schwan, 1966; Fuhr, 1985; Foster et al., 1992; Wang et al., 1993).

Recent measurements of electrorotation at low frequencies showed that the equivalence between impedance and electrorotation, which holds for the Pauly-Schwan and Maxwell-Wagner dispersion range (β-dispersion), does not occur in the α-dispersion range (Arnold et al., 1987; Zhou et al., 1995; Burt et al., 1996; Maier, 1997). Impedance measurements of the low frequency dielectric dispersion indicate a decreasing dielectric permittivity of the suspension with increasing frequency (Kijlstra, 1992, Kijlstra et al., 1993), which should be in the framework of the traditional concept consistent with particle rotation against the external field. Instead, cofield rotation is observed.

It is now widely assumed that the α-dispersion is a result of concentration polarization of the electric double layer (Shilov and Dukhin, 1970b). Electric field-induced electrolyte concentration variations around the particle give rise to asymmetries of the electric double layer. The low frequency dielectric dispersion was calculated assuming a thin double layer (Shilov and Dukhin, 1970a; Shilov and Dukhin, 1970b; Fixman, 1983). An additional generalization for thick double layers being not in local equilibrium was achieved by DeLacey and White (1981).

The relaxation time of concentration polarization can be attributed to the diffusion time over a distance comparable to the particle radius. This estimation of the relaxation time is in good agreement with the frequency range for the α-dispersion.

Received for publication 28 August 1997 and in final form 18 December 1997.

Address reprint requests to Dr. H. Bäumler, Institute of Transfusion Medicine, Charité, D-10098 Berlin, Germany. E-mail: baeumler@rz.charite.hu-berlin.de

0006-3495/98/04/2114/07 $2.00

Concentration polarization influences the distribution of polarization charges and hence, determines the total induced dipole moment of the particle together with its double layer. Yet, the attempt to explain the electrorotation behavior only on the basis of the induced total dipole moment was not successful. The rotation direction was wrongly predicted. As it will be explained below, significant progress in the understanding of low frequency electrorotation (LFER) was achieved when Grosse and Shilov (1996) realized that in addition to the total torque acting on the particle together with its double layer, a motion of the outer part of the double layer relative to the particle can also cause rotation.

LFER studies have so far not been given much attention in the field of biology, although its existence for even living cells (Hu et al., 1990; Paul et al., 1993) and liposomes (Wicher et al., 1987) has been shown. Polystyrene latices covered by an biopolymer film (Zhou et al., 1995; Burt et al., 1996) have been shown to undergo rotation in the low frequency range.

To test the predictions of Grosse and Shilov (1996), we conducted electrorotation measurements of glutaraldehyde-treated red blood cells (Neu et al., 1997). These particles are stable over a large range of ionic strength and observe α-dispersion.

MATERIALS AND METHODS

Red blood cell (RBC) preparation

After centrifugation of RBCs from fresh human blood, the buffy coat and plasma were removed. Then the RBCs were washed twice in phosphate-buffered saline, pH 7.4, (containing 5.8 mM phosphate buffer, 150 mM NaCl, and 5.59 mM KCl) at 20°C. Neuraminidase from *Vibrio cholerae* (Sigma) was used to release the *N*-acetylneuraminic acid (sialic acid) from the RBC surface. One hundred μl of RBC concentrate was added into 900 μl of incubation solution (pH 5.5, 110 mM NaCl, 20 mM $CaCl_2$) containing 0, 2, and 5 μl of 1 unit neuraminidase. These samples were slightly agitated at 37°C. After 1 h, the enzymatic treatment of cells was interrupted adding 9 ml of phosphate-buffered saline at 4°C. Three subsequent washings in phosphate-buffered saline followed. The neuraminidase-treated RBCs as well as the untreated RBCs were fixed by means of glutaraldehyde with a final concentration of 2% for 60 min at 20°C. After fixation, the RBCs were washed three times in phosphate-buffered saline of low conductivity (<10 mS/m) and resuspended in measuring solutions of various conductivities at a hematocrit of 0.1%.

Electrophoretic mobility measurements

The electrophoretic mobility measurement was measured by means of an OPTON cytopherometer (Zeiss, Oberkochen, Germany) as well as by using a prototype of the electrophoretic cell/particle analyzer Electrophor (Hasotec, Rostock). Details of the measuring equipment are given elsewhere (Grümmer et al., 1996).

Electrorotation measurements

Cell electrorotation was recorded by means of a video microscope system. The needle electrode tip separation distance was 1 mm. The chamber volume was 850 μm^3. A computer controlled generator (FOKUS, Giesenhorst, Germany) provides four 90°-phase-shifted, symmetrical square-wave signals in two separate frequency ranges: 10–2000 Hz and 0.26 kHz to 32 MHz. The conductivity of the suspension was measured before and after each experiment. In the case that during the experiment the conductivity slightly increased, the final conductivity was given and used as a parameter for constructing the theoretical curves. The electrorotation spectrum was recorded from 3–8 sedimented RBC. They rotated around their small semiaxis. Measurements were conducted at room temperature (22°C). The viscosities were determined by a means of a capillary viscosimeter.

Qualitative description of the LFER mechanism

The theory of LFER is rather complex (Grosse and Shilov, 1996). So far, a qualitative picture of the mechanism has not been put forward. Hence, it is useful to provide an illustration of the mechanism of concentration polarization together with the nature of the developing electroosmotic component of the particle rotation. Fig. 1 *a* illustrates the concentration polarization. A negatively charged particle is assumed. We consider the particle charge being immobile. The external electric field produces a cation migrative current through the double layer region around the particle. This creates a cation concentration excess and depletion, respectively, at the two opposing sites of the particle. Near the particle surface, deviations of the electrolyte concentration from the bulk are produced due to anion electrodiffusion. Thus in Fig. 1 *a*, the double layer at the upper half of the particle is compressed, whereas along the opposite particle hemi-

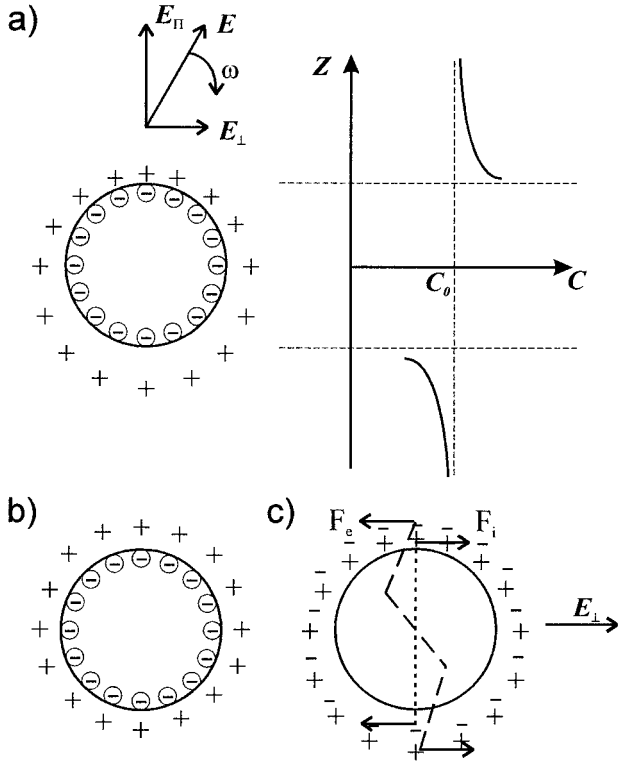

FIGURE 1 Schematic of the charge and concentration variations of a negatively charged particle caused by a rotating electric field and the nature of the electroosmotic component of low frequency electrorotation. (*a*) Representation of the charge distribution around a particle in the presence of a rotating field and the respective cation concentration changes *c* produced by the field-induced electric current flow and diffusion. *z* denotes the axis in phase with the produced concentration changes. (*Upper schema*) Decomposition of the rotating field vector into its two components. (*b*) Equilibrium charge distribution around a spherical particle. (*c*) Deviation of the charge distribution from equilibrium. Illustration of the two electroosmotic driving forces producing the torque.

sphere the decrease of electrolyte concentration causes an expansion of the diffuse part of the double layer. The corresponding concentration changes are illustrated in the coordinate system next to the particle figure. C_0 denotes the equilibrium bulk concentration of cations. The rotating electric field vector can be split into two components: one in-phase with the produced concentration changes $E_{\|}$, and one perpendicular component $E_{\perp}$, which as shown below produces the electroosmotic slip velocity in the Debye atmosphere.

Fig. 1 *b* illustrates the equilibrium ion distribution around the particle in the absence of an external field. This distribution is symmetrical and thus cannot give rise to any rotational motion upon interaction with the field. To find the deviation of the ion distribution from equilibrium it is sufficient to subtract the equilibrium distribution from the field-induced ion distribution in Fig. 1 *a*. The resulting nonequilibrium component of the net ion distribution depicted in Fig. 1 *a* is shown in Fig. 1 *c*. At the top and the bottom of the particle (with regard to the *z* axis shown in Fig. 1 *a*), the Debye atmosphere may be considered to be composed of two shells of opposite charges. It is here in which the perpendicular component of the external rotating field upon interaction with the spatially distributed charges produces two equal in magnitude but oppositely directed volume forces, F_e and F_i. These forces cause the electroosmotic slip. In addition, there is the counterfield directed torque caused by the interaction of the induced dipole moment with the external field, acting upon the whole system consisting of the particle together with the Debye atmosphere (not shown).

Let us now estimate the magnitude and the direction of the electroosmotic and the induced dipole moment-associated torque. The latter torque, M_d, may be estimated as:

$$M_d = Q\delta E_{\perp} \tag{1}$$

Here Q denotes the total charge of the particle in equilibrium. δ is the amplitude of variation of the double layer thickness. Correspondingly, the counterfield dipole-related rotation speed, Ω_d, is found considering the Stokes friction force:

$$\Omega_d = \frac{Q\delta E_{\perp}}{8\pi\eta a^3} \tag{2}$$

η is the medium viscosity and a is the particle radius.

The magnitude of the two electroosmotic torques M_e and M_i are

$$M_e = Q(a + \delta)E_{\perp} \tag{3}$$

$$M_i = Q\delta E_{\perp} \tag{4}$$

These two oppositely directed torques are considered as being applied to two different shells, one with radius a and the other with the radius $a + \delta$. Hence, the rotational speed of the electroosmotic slip becomes

$$\Omega_{osm} = \Omega_i - \Omega_e = \frac{QE_{\perp}}{8\pi\eta}\left[\frac{1}{a^2} - \frac{1}{(a + \delta)^2}\right] \tag{5}$$

Taking into account, $\delta \ll a$, we finally obtain

$$\Omega_{osm} = \frac{2Q\delta E_{\perp}}{8\pi\eta a^3} \tag{6}$$

This estimation reveals that the new electroosmotic component of the rotation speed predominates the induced dipole field interaction mediated electrorotation (Eq. 1), provided the condition $\delta \ll a$ holds.

The electroosmotic nature of the generated torque implies that the electroosmotic component of rotation does not create a liquid rotation outside the Debye atmosphere. From this consideration follows that a long range hydrodynamic interaction between rotating particles caused by the electroosmotic component of the torque cannot exist.

The complete underlying theory is given by an analytical solution too long and too complex to be included here (Grosse and Shilov, 1996). Therefore, we reproduce only the final result for the angular frequency of particle rotation Ω:

$$\Omega = -\frac{\epsilon E^2}{2\eta}\left[H + \frac{1}{z}\tanh\left(\frac{ze\zeta}{2kT}\right)(1 - K_{d\infty})\right] \frac{3z(R^+ - R^-)AW^2(W + 1)/2}{W^2(AW + B)^2 + B^2(W + 1)^2} \tag{7}$$

The first term in the angular brackets H represents the rotation caused by dipole field interaction. It is a complex function of the ζ-potential, the ion diffusion coefficients and charge numbers z, and of the Debye length. The second term describes the electroosmotic component of the total angular speed. It depends on the ζ-potential, the ion diffusion coefficients and charge numbers, and on the Debye length. W^2 is the dimensionless external field frequency scaled by the characteristic time of dispersion. $R^{+/-}$, A, and B are complex functions of the ζ-potential, the ion diffusion coefficients and charge numbers, and of the Debye length. Grosse and Shilov (1996) showed that the two terms within the angular brackets always have opposite signs. For low values of the ζ-potential, the electroosmotic term is the larger of the two so that the particle rotates in the same direction as the field. For high values of the ζ-potential, the electroosmotic term becomes small relative to the induced dipole field interaction term H. The explanation is that with increasing ζ-potential the associated increase of the surface conductance causes a decrease of the tangential component of the applied electric field, which is the driving force for the electroosmotic flow.

As the dissipation of the polarization charges is determined by ion diffusion, the characteristic time of this relaxation process is given by the particle size and the ion diffusion coefficients and, hence, should be only weakly dependent on the external conductivity. Consequently, the position of the peak of the LFER spectrum should be largely independent of the external conductivity.

RESULTS AND DISCUSSION

Glutaraldehyde treatment removes the majority of positive amino groups from the surface, thus keeping the ζ-potential at high negative values upon reduction of ionic strengths. Moreover, the treatment cross-links the proteins and destroys the lipid membrane (Heard and Seaman, 1961). The result is a highly stable particle composed of a matrix of polyelectrolytes with a well known structure and surface composition. The charge density is also well known (Donath et al., 1996a). Neuraminidase treatment before the glutaraldehyde fixing can be used to control the surface charge density without affecting other particle parameters significantly (Luner et al., 1975; Marchesi and Furthmayr, 1976). The disadvantage of the fixed red cell model for testing the new theory is that the surface charges are distributed within a layer of a thickness of the order of a few nanometers. The high ζ-potential, however, ensures a large surface conductance that is the necessary condition for the existence of a well pronounced α-dispersion.

In Fig. 2, we show the LFER spectrum recorded as a function of the electrolyte conductivity. The characteristic feature of all curves is the existence of a maximum of the rotation speed in the range of ~50 Hz. The position of the maximum is only weakly dependent on conductivity. The direction of the rotation is cofield. Another experimental finding is that the rotation speed attains a maximum as a function of electrolyte conductivity. A comparison of the

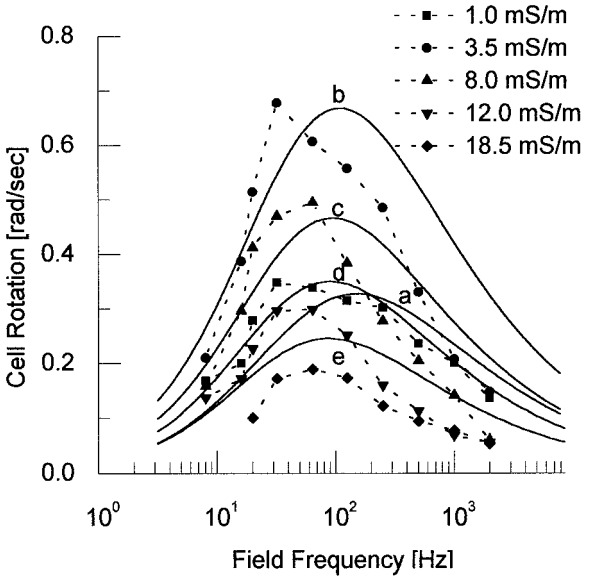

FIGURE 2 Comparison of theoretical and experimental low frequency rotation spectra of fixed red blood cells at different external conductivities. For the theoretical curves, a surface charge density of 0.038 C/m^2 and a cell radius of 3.92 μm was assumed. Conductivities are provided in the graph.

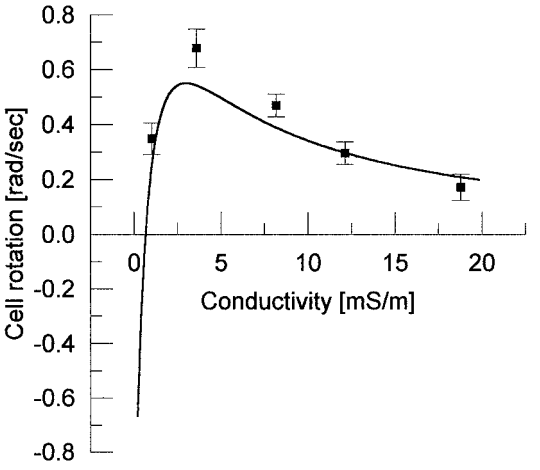

FIGURE 3 Frequency of the cell rotation as a function of the external conductivity at an external field frequency of 32 Hz (for additional details see Fig. 2). The fitted amplitude scaling factor was 1.22.

rotation speeds above 100 Hz indicates a broadening of the rotation speed toward higher frequencies for very low ionic strength. The theoretical curves in Fig. 2 were drawn according to Grosse and Shilov (1996) assuming a surface charge density of 0.038 C/m^2 and a red cell radius of 3.92 μm (Georgieva et al., 1989). The electrolyte concentration was recalculated from the conductivity data using ion mobility data for Cl^- and K^+ (Dobos, 1975). The overall agreement between theory and experiment is evident. The speed and the direction of the cell rotation as well as the maximum of the rotation speed are well described. However, the position of the theoretical maxima does not precisely fit the experimental curves. There is a systematic shift toward higher frequencies. One reason for this behavior could be the fact that the shape of the investigated cells are not spherical as theoretically assumed.

The charge density assumed was slightly higher than expected from the biochemical composition. After fixing with glutaraldehyde, there should be 0.029 C/m^2 (Donath et al., 1996a). Instead it was necessary to assume a value of 0.038 C/m^2 to fit the data in Fig. 2. We attribute this difference to the spatial nature of the cell surface charge distribution. The theoretical model assumes a flat distribution. In the situation of a spatial distribution, the surface conductivity is larger than if the same surface charge would be distributed in a plane. This is the result of the larger convective contribution to the surface conductivity caused by finite electrolyte flow in the charged layer.

When plotting the rotation at a given frequency versus the conductivity of the solution (Fig. 3), again, an overall agreement between theory and the experimental data can be observed. A small deviation of the theoretical curve from experimental data may again be attributed to deviations in size and shape of the cells.

The influence of the surface charge density on the LFER was also tested. The surface charge was partly removed by means of a neuraminidase treatment before the glutaraldehyde fixation. The reduction of the electrophoretic mobility in the low ionic strength region after neuraminidase treatment ranged between 40 to 60% of the control. As a consequence of the spatial nature of the surface charge distribution and the dynamic response of the surface charge arrangement with changing electric potential and, finally, because of the large influence of surface conductivity on mobility in the low ionic strength region, there is no direct proportionality between the mobility and the charge density. The resulting LFER spectra are shown in Fig. 4. It is obvious that in this conductivity range the rotation speed was decreased with decreasing surface charge density. The fit of the rotation data indicates a larger reduction of the surface charge than inferred from electrophoretic measurements alone.

The theoretical peak positions match the experimentally observed peaks. An important feature of the human erythrocytes is the existence of a variety of shapes. Naturally, the flat shape of a discocyte will be consistent with a smaller average distance between cells and the supports as compared with, for example, echinocytes. As the treatment with neuraminidase influences the surface structure of the glycoprotein layer (Donath et al., 1996a) and also the shape of erythrocytes, it could be that the friction between the cell and the support has also changed, which would explain the different amplitudes observed in Fig. 4 (when compared with Fig. 2).

The Maxwell-Wagner peak of the fixed erythrocytes was measured as a function of electrolyte concentration. The data together with theoretical plots are provided in Fig. 5. The rotation speed in the MHz region was small. It changed from a positive rotation at very low electrolyte concentra-

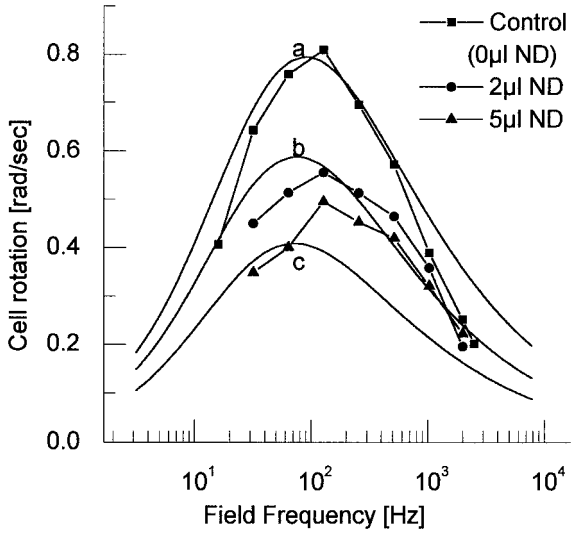

FIGURE 4 Experimental and theoretical (*solid lines*) low frequency rotation spectra of fixed red blood cells with different surface charges. The *insert* provides neuraminidase amounts (see Materials and Methods). All spectra were measured at an external conductivity of 2.3 mS/m. For the theoretical curves, a cell radius of 3.92 μm and an amplitude scaling factor of 2.05 was used. The surface charge densities were 0.038 C/m^2 (*a*), 0.013 C/m^2 (*b*), and 0.008 C/m^2 (*c*).

tion to negative rotation speeds upon increasing the bulk conductivity. The position of the peak shifted with increasing conductivity toward higher frequencies.

To construct the theoretical curves, the model of Pastushenko et al. (1985) was used. It is applicable to spherically symmetrical particles with an arbitrary radial profile of the dielectric and conductivity parameters. The comparison of the theoretical curves with the experimental data suggests that the fixed cells behave as slightly conducting particles. This picture was largely consistent with the theoretical

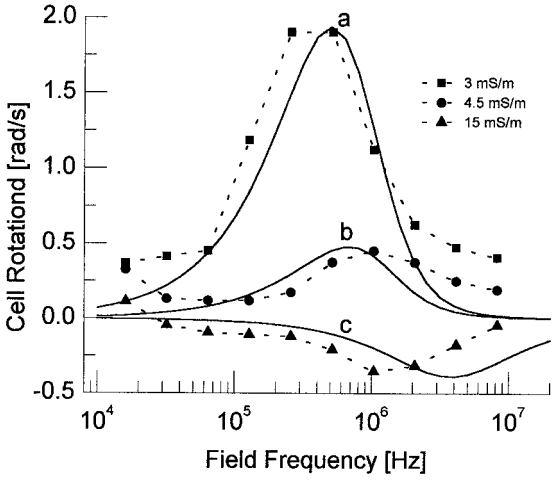

FIGURE 5 Comparison of theoretical and experimental high frequency rotation spectra of fixed red blood cells at different external conductivities. For the theoretical data conducting spheres with 0.3 mS/m (*a*), 0.45 mS/m (*b*) and 1.47 mS/m (*c*) surrounded by conducting shells with 0.47, 0.56, and 1.6 mS/m, respectively. The interior and bulk dielectric constant was 78.

rotation of a weakly conducting sphere surrounded by a conducting shell. The conductance of the shell should be larger than the bulk value to obtain cofield rotation. Counterfield rotation would be consistent with a shell conductivity less than the bulk conductivity. We additionally assumed the dielectric constant to be equal to the bulk water value of 78. At bulk conductivities of 3 and 4.5 mS/m, the particle's conductivity has to be larger than the bulk one to result in cofield rotation. At higher bulk conductivities the smaller core conductivity of the particle caused a reversal of the direction of rotation. This picture is consistent with a behavior of a polyelectrolyte matrix. At lower bulk conductivities we obviously see the surface (and partly volume) conductance of the polyelectrolyte matrix, whereas at higher bulk conductivities the decrease of the surface potential together with ion exclusion from the polyelectrolyte matrix result in a decrease of the particle conductance compared with the bulk.

It was inferred from the rotation of native erythrocytes that the cytoplasmic dielectric constant is of the order of 50. To explain the above date it was, however, necessary to assume a value of 78. This could well be a result of the glutaraldehyde-induced cross-linking of the proteins. This should result in an increased electrical coupling. This can explain the increase in the dielectric constant (Bäumler et al., 1988).

It is worth noting that no evidence of a remaining lipid membrane was seen in the rotation spectrum. Additionally, the use of a spherical particle model cannot fully describe the peak positions of erythrocytes. This could be the reason for the shift between the theoretical and experimental peaks in Fig. 5. Models for ellipsoidal particles seem to be more appropriate (Jones, 1995; Müller et al., 1993). Unfortunately, there is currently no theory of LFER for ellipsoidal particles available.

To provide additional evidence for the overwhelming electroosmotic contribution to rotation in the low frequency range, we illustrate in Fig. 6 the often observed "dancing" pairs of cells. Two cells attracted toward each other by polarization forces and thus located at a close distance rotate independently into the same direction as the rotating field (denoted by Ω). The speed of each of these cells does not

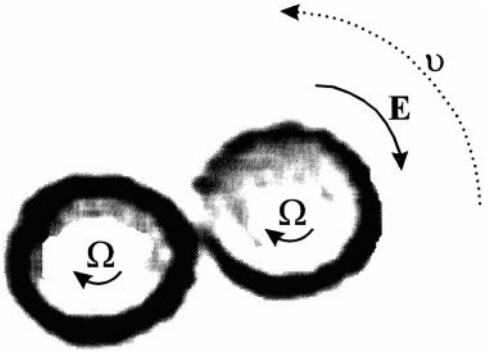

FIGURE 6 Schematic of a pair of rotating cells.

differ from a single rotating cell. The whole pair may very slowly rotate into the opposite direction (denoted by ν).

Obviously, there is no appreciable hydrodynamic interaction between the two cells, although their separation distance is quite small. This can only be understood if assuming a rotation associated flow field, the range of which is shorter than the separation gap width. Such a flow field is characteristic for the electroosmotic component of rotation. This results from the fact that the curl of any electroosmotic flow is zero outside the double layer. Such a flow field cannot permit hydrodynamic interactions between the cells separated at distances significantly larger than the Debye length (Bäumler and Donath, 1987; Donath et al., 1996b). We believe this is convincing evidence for the electroosmotic nature of the rotation (Grosse and Shilov, 1996). The flow field caused by the rotation caused by the electric field dipole interaction component of the net rotation has a dissipative nature and gives rise to cell-cell interaction. This explains the very slow counterfield rotation of the pair sometimes seen.

CONCLUSION

It has been shown that fixed red blood cells show electrorotation in the 10^1- to 10^3-Hz region. The rotation behavior is consistent with the prediction of Grosse and Shilov (1996). In contrast to the Pauly-Schwan and Maxwell-Wagner range of rotation (β-dispersion) in which membrane or bulk properties such as dielectric constant and conductivity are responsible for electrorotation behavior, the LFER is caused by the surface conductance and the surface charge of the particles. The equivalence between electrorotation and impedance measurements breaks down as a consequence of the electroosmotic component of LFER.

The available theory describes the standard model of an electric double layer around a spherical particle. New theoretical efforts are necessary to overcome this restriction and to develop models applicable for particles with various shapes and soft surfaces.

In contrast to the high frequency range, the LFER theory for the standard model has only one adjustable parameter, either the surface charge density or the ζ-potential. Both parameters can be assessed independently. Thus, the comparison between LFER measurements and other methods can identify the contribution of, for example, the anomalous surface conductance or hairy layers.

In summary, the achievements in the experimental characterization and theoretical description of the low frequency electrorotation should give rise to additional applications in this field.

We kindly acknowledge the technical assistance of B. Franz and discussion with Dr. E. Hessel (Institute of Biophysics, Charité) concerning the Neuraminidase treatment. This work was supported by Grants Ba 1545/1 and Kn 385/1–2 of the Deutsche Forschungsgemeinschaft. R. Georgieva acknowledges the support of the TEMPUS EU exchange program.

REFERENCES

Arnold, W. M., H. P. Schwan, and U. Zimmermann. 1987. Surface conductance and other properties of latex particles measured by electrorotation. *J. Phys. Chem.* 91:5093–5098.

Arnold, W. M., and U. Zimmermann. 1982. Rotating-field-induced rotation and measurement of the membrane capacitance of single mesophyll cells of *Avena sativa. Z. Naturforsch.* 37C:908–915.

Arnold, W. M., and U. Zimmermann. 1988. Electro-rotation: development of a technique for dielectric measurements on indiviual cells and particles. *J. Electrostatics* 21:151–191.

Bäumler, H., and E. Donath. 1987. Does dextran indeed significantly increase the surface potential of human red blood cells? *Stud. Biophys.* 120:113–122.

Bäumler, H., I. Djenev, S. Iovtchev, R. Petrova, and D. Lerche. 1988. Polarizability of human red blood cells and conformational state of glycocalyx. *Stud. Biophys.* 125:45–51.

Burt, J. P. H., K. L. Chan, D. Dawson, A. Patron, and R. Pethig. 1996. Assays for microbial contamination and DNA analysis based on electrorotation. *Ann. Biol. Clin.* 54:253–257.

DeLacey, E. H. B., and L. R. White. 1981. Dielectric response and conductivity of dilute suspensions of colloidal particles. *J. Chem. Soc., Faraday Trans.* 277:2007–2039.

Dobos, D. 1975. Electrochemical Data. Akademiai kiado, Budapest.

Donath, E., A. Budde, E. Knippel, and H. Bäumler. 1996a. "Hairy surface layer" concept of electrophoresis combined with local fixed surface charge density isotherms: application to human erythrocyte electrophoretic fingerprinting. *Langmuir.* 12:4832–4839.

Donath, E., A. Krabi, G. Allan, and B. Vincent. 1996b. A study of polymer depletion layers by electrophoresis: the influence of viscosity profiles and the nonlinearity of the Poisson-Boltzmann equation. *Langmuir.* 12:3425–3430.

Donath, E., V. Pastushenko, and M. Egger. 1990. Dielectric behavior of the anion-exchange protein of human red blood cells: theoretical analysis and comparison to electrorotation data. *Bioelectrochem. Bioenerg.* 23: 337–360.

Dukhin, S. S., and V. N. Shilov. 1974. Dielectric Phenomena and the Double Layer in Disperse Systems and Polyelectrolytes. Wiley, New York.

Egger, M., and E. Donath. 1995. Electrorotation measurements of diamide-induced platelet activation changes. *Biophys. J.* 68:364–372.

Fixman M.. 1983. Thin double layer approximation for electrophoresis and dielectric response. *J. Chem. Phys.* 78:1483–1491.

Foster, K. R., F. A. Sauer, and H. P. Schwan. 1992. Electrorotation and levitation of cells and colloidal particles. *Biophys. J.* 63:180–190.

Fuhr, G. 1985. Über die Rotation Dielektrischer Körper in Rotierenden Feldern. Dissertation, Humboldt-Universität zu Berlin, Berlin.

Georgieva, R., E. Donath, and R. Glaser. 1989. On the determination of human erythrocyte intracellular conductivity by means of electrorotation-influence of osmotic pressure. *Stud. Biophys.* 133:185–197.

Gimsa, J., T. Müller, Th. Schnelle, and G. Fuhr. 1996. Dielectric spectroscopy of single human erythrocytes at physiological ionic strengths: dispersion of the cytoplasm. *Biophys. J.* 71:498–506.

Grosse, C., and V. N. Shilov. 1996. Theory of the low-frequency electrorotation of polystyrene particles in electrolyte solution. *J. Phys. Chem.* 100:1771–1778.

Grümmer, G., E. Knippel, A. Budde, H. Brockmann, and J. Treichler. 1996. An electrophoretic instrumentation for the multi-parameter analysis of cells and particles. *Instr. Sci. Techn.* 23:265–276.

Heard, D. H., and G. V. F. Seaman. 1961. The action of lower aldehydes on the human erythrocyte. *Biochim. Biophys. Acta.* 53:366–374.

Hu, X., W. M. Arnold, U. Zimmermann. 1990. Alterations in the electrical properties of T and B lymphocyte membranes induced by mitogenic stimulation. Activation monitored by electro-rotation of single cells. *Biochim. Biophys. Acta.* 1021:191–200.

Huang, Y., X. B. Wang, R. Hölzel, F. F. Becker, and P. R. Gascoyne. 1995. Eletrorotational studies of the cytoplasmatic dielectric properties of friend murine erythroleukaemia cells. *Phys. Med. Biol.* 40:1789–1806.

Jones, T. B. 1995. Electromechanics of particles. Cambridge University Press, Cambridge, New York, Melbourne.

Kijlstra, J. 1992. Double layer relaxation in colloids. Thesis. Agricultural University Wageningen.

Kijlstra, J., H. P. van Leeuwen, J. Lyklema. 1993. Low-frequency dielectric relaxation of hematite and silica sols. *Langmuir.* 9:1625–1633.

Luner, J. L., P. Sturgeon, D. Szklarek, and D. T. McQuiston. 1975. Effects of proteases and neuraminidase on RBC surface charge and agglutination. *Vox. Sang.* 28:184–199.

Maier, H. 1997. Electrorotation of colloidal particles and cells depends on surface charge. *Biophys. J.* 73:1617–1626.

Marchesi, V. T., and H. Furthmayr. 1976. The red cell membrane. *Annu. Rev. Biochem.* 45:667–698.

Müller, T., L. Küchler, G. Fuhr, T. Schnelle, and A. Sokirko. 1993. Dielektrische Einzelzellspektroskopie an Pollen verschiedener Waldbaumarten - Charakterisierung der Pollenvitalität. *Silvae Genet.* 42: 311–322.

Neu, B., R. Georgieva, H. Bäumler, V. N. Shilov, E. Knippel, and E. Donath. 1997. Low-frequency dispersion of surface conducting particles as measured by means of electrorotation. *Colloids Surf.* (in press).

Pastushenko, V. Ph., P. I. Kuzmin, and Yu. A. Chizmadshev. 1985. Dielectrophoresis and electrorotation: a unified theory of spherically symmeterical cells. *Stud. Biophys.* 110:51–57.

Paul, R., K. V. I. S. Kaler, and T. B. Jones. 1993. A nonequilibrium statistical mechanical calculation of the surface conductance of the electrical double layer of biological cells and its application to dielectrophoresis. *J. Phys. Chem.* 97:4745–4755.

Pauly, H., and H. P. Schwan. 1966. Dielectric properties and ion mobility in erythrocytes. *Biophys. J.* 6:621–639.

Shilov, V. N., and S. S. Dukhin. 1970a. The theory of low frequency dielectric permeability of suspensions of spherical colloidal particles caused by double layer polarization. *Kolloidn. Zh.* 32:117–123.

Shilov, V. N., and S. S. Dukhin. 1970b. The theory of polarization of diffuse part of thin double layer of spherical particles in alternating fields. *Kolloidn. Zh.* 32:293–300.

Sukhorukov, V. L., and U. Zimmermann. 1996. Electrorotation of erythrocytes treated with dipicrylamine: mobile charges within the membrane show their "signature" in rotational spectra. *J. Membr. Biol.* 153: 161–169.

Wang, X.-B., Y. Huang, P. R. C. Gascoyne, F. F. Becker, R. Hölzel, R. Pethig. 1994. Changes in Friend murine erythroleukaemia cell membranes during induced differentiation determined by electrorotation. *Biochim. Biophys. Acta.* 1193:330–344.

Wang, X.-B., Y. Huang, R. Hölzel, J. P. H. Burt, and R. Pethig. 1993. Theoretical and experimental investigations of the interdependence of the dielectric, dielectrophoretic and electrorotational behaviour of colloidal particles. *J. Phys. D: Appl. Phys.* 26:312–322.

Wicher, D., J. Gündel, and H. Matthies. 1987. Electrorotation of liposomes in the α - and β - dispersion range. *Stud. Biophys.* 119:103–104.

Zhou, X.-F., G. H. Marx, R. Pethig, and I. M. Eastwood. 1995. Differentiation of viable and non-viable bacterial biofilms using electrorotation. *Biochim. Biophys. Acta.* 1245:85–93.